

Soft Matter

Accepted Manuscript



This is an *Accepted Manuscript*, which has been through the Royal Society of Chemistry peer review process and has been accepted for publication.

Accepted Manuscripts are published online shortly after acceptance, before technical editing, formatting and proof reading. Using this free service, authors can make their results available to the community, in citable form, before we publish the edited article. We will replace this *Accepted Manuscript* with the edited and formatted *Advance Article* as soon as it is available.

You can find more information about *Accepted Manuscripts* in the [Information for Authors](#).

Please note that technical editing may introduce minor changes to the text and/or graphics, which may alter content. The journal's standard [Terms & Conditions](#) and the [Ethical guidelines](#) still apply. In no event shall the Royal Society of Chemistry be held responsible for any errors or omissions in this *Accepted Manuscript* or any consequences arising from the use of any information it contains.

ARTICLE

Fast Formation of Superhydrophobic Octadecylphosphonic Acid (ODPA) Coating for Self-cleaning and Oil/Water Separation

Cite this: DOI: 10.1039/x0xx00000x

Chunai Dai,^{ab} Na Liu,^a Yingze Cao,^a Yuning Chen,^a Fei Lu^a and Lin Feng^{*a}Received 22th July 2014,
Accepted 00th July 2014

DOI: 10.1039/x0xx00000x

www.rsc.org/

A simple and fast method to prepare robust superhydrophobic octadecylphosphonic acid (ODPA) coating on oxidized copper mesh for self-cleaning and oil/water separation is reported here. The substrate of the copper mesh was first oxidized by simple immersion in an aqueous solution of 1.0 M NaOH and 0.05 M K₂S₂O₈ at room temperature for 30 min, which was then covered with micro- and nanoscale Cu(OH)₂ in the surface. Subsequently, the oxidized copper mesh was immersed in 2 × 10⁻⁴ M octadecylphosphonic acid/tetrahydrofuran (ODPA/THF) solution, an ODPA coating prepared. The ODPA coating formation process takes place rapidly, almost in 1 second, which makes the as-prepared mesh exhibit superhydrophobicity with the water contact angle of approximately 158.9° and superoleophilicity with the oil contact angle of 0°. Then the as-prepared mesh has self-cleaning effect and can be repeatedly used to separate a series of oil/water mixtures like gasoline/water, diesel/water, etc. efficiently. Interestingly, straightforward oxidation of a copper substrate produces a "water-removing" type oil/water separation mesh with underwater superoleophobicity, and ODPA coating on the oxidized copper mesh produces an "oil-removing" type oil/water separation mesh with superhydrophobicity and superoleophilicity. This interesting conversion just results from a small amount of ODPA used and takes place so rapidly.

1 Introduction

Functional solid surfaces are versatile and have many potential applications in the fields of non-wetting surfaces, corrosion inhibition, lubrication, monolayer lithography, biocompatible surfaces, etc.^{1,5-7} Because of the serious water pollution like oil spill accidents, oily wastewater from industries, etc., functional solid surfaces with special wetting behaviour used for oily wastewater treatment has attracted more attention. In 2004, L. Jiang et al.⁸ for the first time reported a Teflon coated mesh with superhydrophobicity and superoleophilicity for separation of oil and water. Then it is known that, thanks to the different interfacial effects of oil and water, functional solid surfaces with special wetting behaviour can be used to design an effective oil/water separation process. Since then novel

functional solid surfaces with special wettability as oil/water separation materials with high efficiency and selectivity have been extensively investigated.⁹⁻²⁶ Accordingly, two types of oil/water separation materials, i.e., the "water-removing" type with superhydrophilicity and superoleophobicity as well as the "oil-removing" type with superhydrophobicity and superoleophilicity have been developed. Various materials such as polytetrafluoroethylene (PTFE)-coated mesh,⁸ kapok,²⁰ polyelectrolyte gels,¹⁰ carbon-based membranes,²¹ polyurethane (TPU) films,²² hierarchical Teflon-coated mesh,²³ graphene-based sponges,²⁴ and collagen-based magnetic nanocomposites²⁵ have been developed as oil-removing materials which can realize filtration or absorption of oils from water. Polyacrylamide (PAM) hydrogel-coated mesh²⁶ and so on have been developed as water-removing material which can selectively filter water from oil/water mixtures. However, for some reasons such as the complicated preparation process or unstable coating, these materials still deserve to be further researched on for practical use. In addition, the conversion between these two kinds of materials is seldom reported. Our group has reported the "water-removing" type oil/water separation material: straightforward oxidation of a copper

^aDepartment of Chemistry, Tsinghua University, Beijing 100084, P. R. China. E-mail: fl@mail.tsinghua.edu.cn

^bSchool of Science, Beijing Jiaotong University, Beijing 100044, P. R. China. E-mail: chadai@bjtu.edu.cn

[†]Electronic Supplementary Information (ESI) available: movies and their description. See DOI: 10.1039/b000000x/

substrate produces an underwater superoleophobic mesh. Water can selectively penetrate through the mesh whereas oil is blocked.²⁷ In the current work, we report that, after facile surface functionalization with octadecylphosphonic acid (ODPA), the above “water-removing” type mesh can be instantly changed to an “oil-removing” type mesh with superhydrophobicity and superoleophilicity, which can also be used for oil/water separation while oil can selectively penetrate through the mesh whereas water is blocked (ESI†). This interesting conversion takes place rapidly and therefore has greater potential in industrial applications.

2 Experimental

2.1 Chemicals

All the chemicals used for the experiments were standard commercial grade. They were used as received without any further purification. The copper mesh substrate used was cleaned with deionized water and acetone. Sodium hydroxide (NaOH, analytical grade) was obtained from Beijing Chemical Co. Ltd of China. Potassium peroxydisulfate ($K_2S_2O_8$, 99.99%), methanol, octadecylphosphonic acid ($CH_3(CH_2)_{17}PO(OH)_2$, ODPA) and tetrahydrofuran (THF) were from Alfa Aesar, Tianjin, China.

2.2 Substrate preparation

The original mesh used as substrate was knitted from copper wires. The mesh was of a 400 mesh size and ultrasonicated sequentially in deionized water and acetone, and then dried at room temperature. Pre-cleaned copper mesh was immersed in an aqueous solution of 1.0 M NaOH and 0.05 M $K_2S_2O_8$ at room temperature for 30 min. Then the oxidized mesh was taken out and washed with deionized water. The obtained mesh turned to blue from the original shiny red colour.

2.3 ODPA coating preparation

ODPA coating on copper surface was produced by liquid phase reaction. The ODPA/THF solution of 2×10^{-4} M was made by dissolving ODPA powder into THF solvent (ODPA/THF solution had to be ultrasonicated in order to completely dissolve the powder). The oxidized copper mesh was immersed into ODPA/THF solution at room temperature under ambient condition for 1 second. Then the as-prepared copper mesh was taken out and dried at room temperature.

2.4 Oil/water separation experiment

The as-prepared mesh was fixed between two Teflon fixtures. Both of the fixtures were attached with a glass tube and placed with a tilt angle of about 15° . The diameter of the glass tube was 30 mm. The oil/water mixture (30 v/v%) was poured onto the mesh. The separation was achieved driven by gravity. The blocked water was collected and the oil content in the water was determined by an infrared spectrometer oil content analyser (CY2000, China).

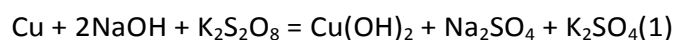
2.5 Instruments and characterization

SEM was performed on a field emission scanning electron microscope (Hitachi S4800, Japan). Infrared spectra were obtained with a Spectrum 100 FTIR spectrometer (Perkin-Elmer, United States). Contact angles were measured on an OCA20 machine (Data-Physics, Germany) at ambient temperature. The X-ray photoelectron spectra (XPS) were acquired by a Scanning X-ray Microprobe (PHI Quantera, ULVAC-PHI, Japan) using an Al $K\alpha$ X-ray source (1486.7 eV).

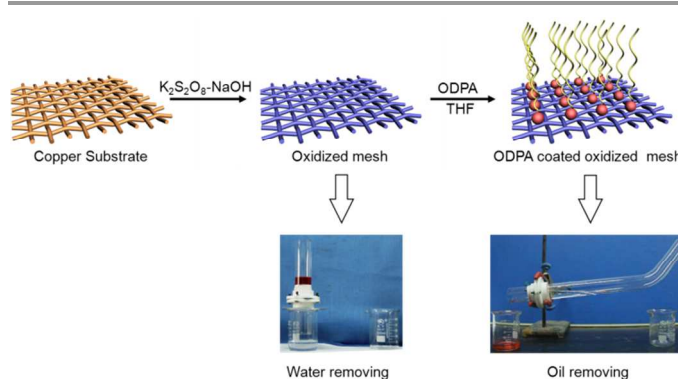
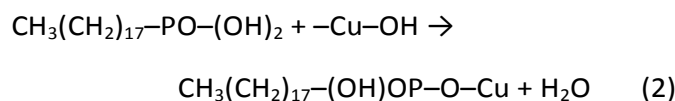
3 Results and discussion

3.1 Proposed mechanism of ODPA coating formation on alkaline-oxidized copper mesh

Scheme 1 is the schematic description of ODPA coating formation on alkaline-oxidized copper mesh. The substrate of the copper mesh was first oxidized by simple immersion in the aqueous solution of 1.0 M NaOH and 0.05 M $K_2S_2O_8$ at room temperature for 30 min. The copper mesh was covered with $Cu(OH)_2$ by alkaline oxidation. The formation of $Cu(OH)_2$ on copper mesh occurs through a simple chemical oxidation process:



Then the oxidized mesh was immersed in 2×10^{-4} M ODPA/THF solution. The polar solvent THF is appropriate vehicle for delivery of ODPA on the oxidized copper mesh because ODPA can be dissolved in THF and the oxidized copper mesh surface is easily wetted by the solution. According to references, the reactive molecule ODPA is a type of self-assembled organic molecule which consists of active head group phosphonic acid that can be chemically adsorbed on the oxidized copper mesh surface and the ODPA coating is a kind of self-assembled monolayer (SAM).²⁸⁻⁴⁵ ODPA interacts with $Cu(OH)_2$ probably through the formation of robust Cu-O-P bonds:



Scheme 1 Schematic description of ODPA coating formation on alkaline-oxidized copper mesh.

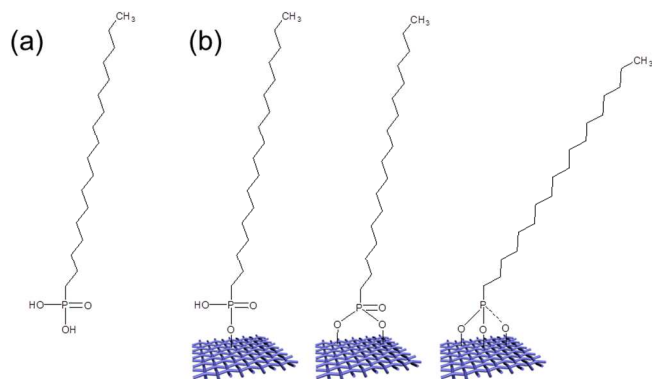
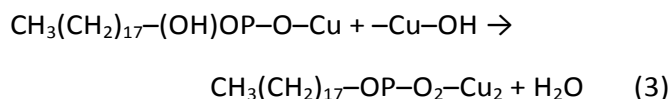


Fig. 1 (a) Chemical structure of ODPA; (b) monodentate, bidentate, and tridentate bonding for ODPA reacted with $\text{Cu}(\text{OH})_2$ -covered copper mesh.



And in accordance with bonding mechanisms reported in the literature,¹ a tridentate reaction is plausible. When an ODPA molecule with both OH groups and the O group is bound to the $\text{Cu}(\text{OH})_2$ -covered copper mesh via monodentate, bidentate, and tridentate bonding, there exist three configurations (Fig. 1). ODPA, when fully extended in the trans zigzag conformation, is a linear-shaped lipid molecule with a length of 2.5 nm.²⁸ If all three oxygen atoms of the phosphonic acid group are attached to the oxidized copper surface, the alkyl chains of the ODPA must be tilted from the surface normal because of tetrahedral bonding angles around P and geometric considerations (assuming that the alkyl chain remains in the fully extended trans zigzag configuration). In ODPA coating, the terminal methyl groups of the alkyl chains are oriented outward, reducing the access of the water drop to the oxidized copper mesh surface. Then the as-prepared mesh showed superhydrophobicity and superoleophilicity, which can be used for oil/water separation.

3.2 Morphology and composition characterization

Fig. 2 shows the SEM images of the copper mesh substrate, the alkaline-oxidized copper mesh, and the ODPA coated alkaline-oxidized copper mesh. The typical image of copper mesh substrate that is knitted by copper wires with pore diameter of approximately 40 μm is shown in Fig. 2a, which indicates that the original mesh has a smooth and clear surface. Fig. 2b is the image of the oxidized mesh showing that the frame of the mesh is wrapped thickly and uniformly by $\text{Cu}(\text{OH})_2$ hairy nanowires. Fig. 2c and d are the images of the ODPA coated oxidized mesh. It can be shown that the ODPA coating does not affect the roughness of the $\text{Cu}(\text{OH})_2$ nanowire-haired copper mesh. FTIR was employed to explore the possible mechanism. Fig. 3a shows the transmission FTIR spectra in the range from 900 to 4000 cm^{-1} for copper mesh substrate (line I), oxidized copper mesh (line II) and ODPA-coated oxidized copper mesh (line III). Fig. 3b shows the infrared spectrum of the C-H stretching region of the ODPA-coated oxidized copper mesh. In Fig. 3a, the peaks at 3298–3303 and 3571–3572 cm^{-1} are ascribed to the

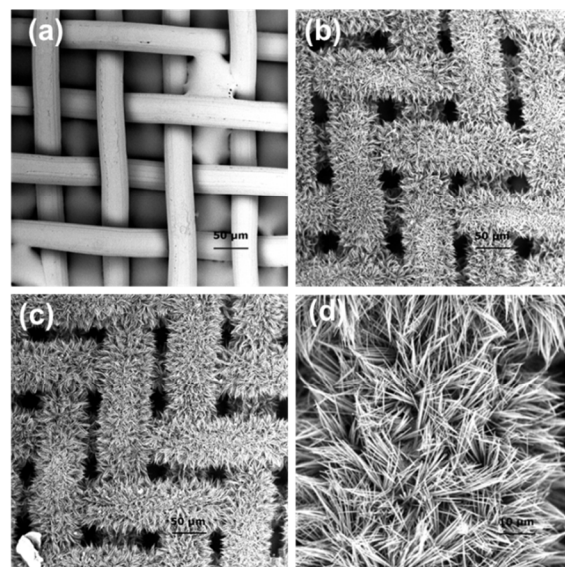


Fig. 2 SEM images of (a) copper mesh as substrate, (b) alkaline-oxidized copper mesh, (c) ODPA coated oxidized copper mesh and (d) ODPA coated oxidized copper mesh with a scale bar of 10 μm .

OH vibration of $\text{Cu}-\text{OH}$ and absorbed H_2O in the sample, which result from alkaline oxidation of the copper mesh. For ODPA coating, generally the ordering of alkyl groups can be assessed from the infrared spectrum using the position of CH_2 stretch. For completely disordered structure, it is close to that of a liquid alkane ($\nu_a \sim 2924 \text{ cm}^{-1}$). For well-ordered structure, it is shifted to lower wavenumber approaching this for crystalline alkane ($\nu_a \sim 2915\text{--}2918 \text{ cm}^{-1}$).⁴⁶ As shown in Fig. 3a and b, the peak frequencies of $\nu_s(\text{CH}_2)$ and $\nu_a(\text{CH}_2)$ for the ODPA coating prepared on the copper mesh are found to be 2851 and 2924 cm^{-1} respectively, indicating that ODPA coating is not well ordered ($\nu_a = 2924 \text{ cm}^{-1}$) probably due to the short immersion time. And because of the small amount of ODPA in the mesh surface, the peaks of 2961, 2971 and 2883 cm^{-1} representing the out-of-plane, in-plane asymmetric methyl stretching mode

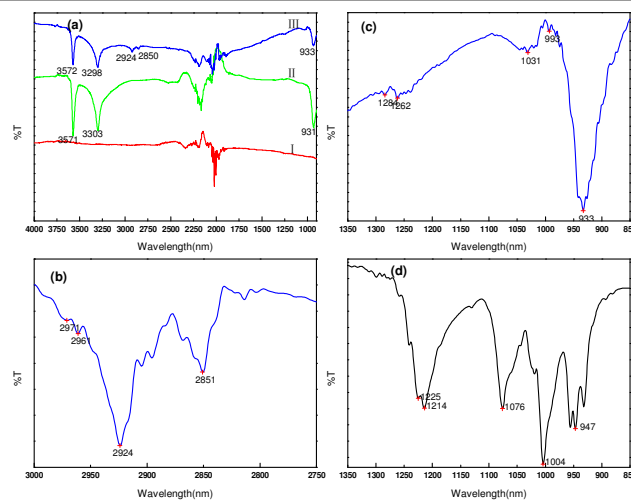


Fig. 3 FTIR spectra of (a) copper mesh substrate (line I), oxidized copper mesh (line II) and ODPA coated oxidized copper mesh (line III); (b) methylene stretching region of ODPA coated oxidized copper mesh; (c) P-O stretching region of ODPA coated oxidized copper mesh, and (d) solid ODPA.

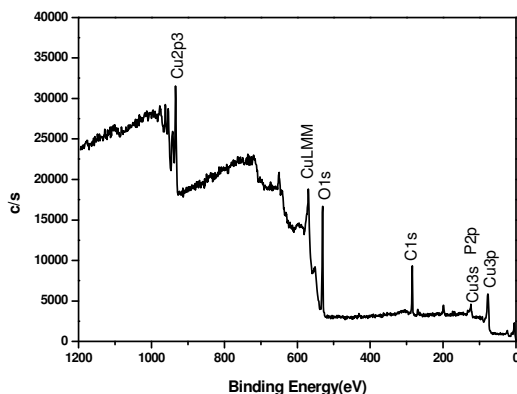


Fig. 4 XPS spectrum conducted on the as-prepared mesh

Table 1 Atomic percent concentration (at%) for the elements Cu, O, C and P and the elemental ratio of C/P quantified from the XPS multiplex of Cu2p3, O1s, C1s, and P2p

Cu	O	C	P	C/P
20.94	42.17	34.73	2.16	16.08

$[v_a(\text{CH}_3)]$ and the symmetric methyl stretching mode $[v_s(\text{CH}_3)]$ are very small in Fig. 3b.⁴⁷ For phosphonic acid, the IR stretch values in the P-O region, which correspond to 1300-950 cm^{-1} , can provide information about the type of bonding of the head group with the substrate. Fig. 3d shows the P-O stretching region of the FTIR spectrum of solid ODP. IR bands at 1225 and 947 cm^{-1} are assigned to $\nu_{\text{P=O}}$ and $\nu_{\text{P-OH}}$ respectively and the bands at 1076 and 1010 cm^{-1} are assigned to the symmetric and asymmetric stretch of ν_{PO_3} . However, because the amount of ODP on the oxidized copper mesh is small, these peaks cannot be clearly presented in P-O stretching region of the FTIR spectrum of the ODP-coated oxidized copper mesh (Fig. 3c), and then the exact binding mode of the ODP to the oxidized copper mesh cannot be concluded only from the FTIR spectra.

So we measured the chemical composition of the as-prepared mesh with XPS to further confirm the successful modification. The basic elements including copper (Cu), oxygen (O), carbon (C), and phosphorus (P) were surveyed by scanning bonding energy from 0 to 1200 eV (Fig. 4). Peaks at 934, 530, 284 and 133 eV labelled in Fig. 4 represent Cu2p3, O1s, C1s and P2p respectively. The chemical surface composition (at%) and elemental ratio (C/P) quantified from the high-resolution core level XPS multiplex performed on the as-prepared mesh are summarized in Table 1. The phosphorus detected in Fig. 4 and Table 1 is an indication of the presence of phosphonate molecule on the mesh surface. In Table 1, the elemental ratio of C/P is 16.08, which approaches the expected value of 18. The small negative deviation from the theoretical ratio value probably stems from the disordered alkyl chains.

3.3 Contact angles measurement

The wettability of the functional solid surface is evaluated through the contact angle (CA). As we reported before, $\text{Cu}(\text{OH})_2$ is a common substance with high surface free-energy, which can easily be wetted by water. After the copper mesh

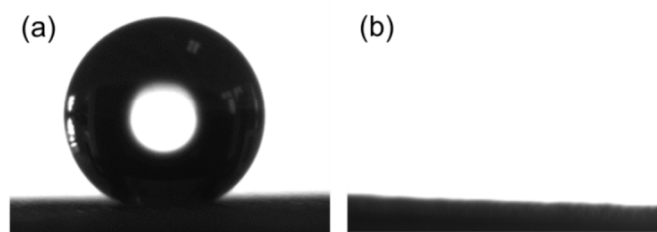


Fig. 5 Wettability of the as-prepared mesh: (a) the photograph of a water droplet (3 μL) on the mesh with a contact angle of $158.9 \pm 1.7^\circ$; (b) the photograph of an oil droplet (1, 2-dichloroethane, 3 μL) spreading and permeating quickly on the mesh.

being oxidized, $\text{Cu}(\text{OH})_2$ with nanoscale structure is introduced, and then the oxidized copper mesh exhibits superhydrophilicity and superoleophilicity in air.³⁸ Herein, we report the wettability change of the oxidized copper mesh after ODP being coated. Actually, it was impossible to measure the water CA of the as-prepared mesh with the sessile method because the ODP surface showed a low adhesion to water. Water droplets either bounced or rolled on the surface, and the latter occurred when there was a slight tilt of $4.8 \pm 0.8^\circ$, indicating that the surface has a very good superhydrophobicity and a small sliding angle of $4.8 \pm 0.8^\circ$. Fig. 5a shows the photograph of a water droplet (3 μL) on the as-prepared copper mesh. It can be shown that the water CA, a value of $158.9 \pm 1.7^\circ$ was observed. By contrast, an oil droplet (1,2-dichloroethane, 3 μL) with a low surface tension spread quickly on the surface and permeated it thoroughly, exhibiting highly oleophilic property with an oil CA of 0° (Fig. 5b). As we know, the wettability of a solid surface is governed by its chemical properties and microstructure. That the superhydrophobic ODP coating can be formed fast is thought to be the result of a combination of the long alkyl chains of ODP and the roughness of $\text{Cu}(\text{OH})_2$ covered.

We investigated the stability of the superhydrophobic ODP coating. After the as-prepared mesh was rinsed with methanol for 5 min, no change was observed in the water contact angle. It indicates that the ODP coating on the alkaline-oxidized copper mesh is robust to some extent.⁴⁰ However, it can be easily understood that the as-prepared mesh is not resistant to strong acid and strong alkali because the superhydrophobic ODP layer itself results from the acid ODP and the alkali $\text{Cu}(\text{OH})_2$.

3.4 Self-cleaning effect

Functional surfaces with very high static water CA and very low sliding angle, similar to the lotus leaf, are well known to have an important application in the field of self-cleaning. To investigate the self-cleaning effect, the as-prepared mesh was contaminated with graphite powders obtained from pencil lead. As shown in Fig. 6, the water droplet adsorbed graphite particles as it moved over the surface from left to right. Contaminants were removed from the surface, demonstrating the lotus leaf-like self-cleaning effect of the as-prepared mesh.⁴⁸

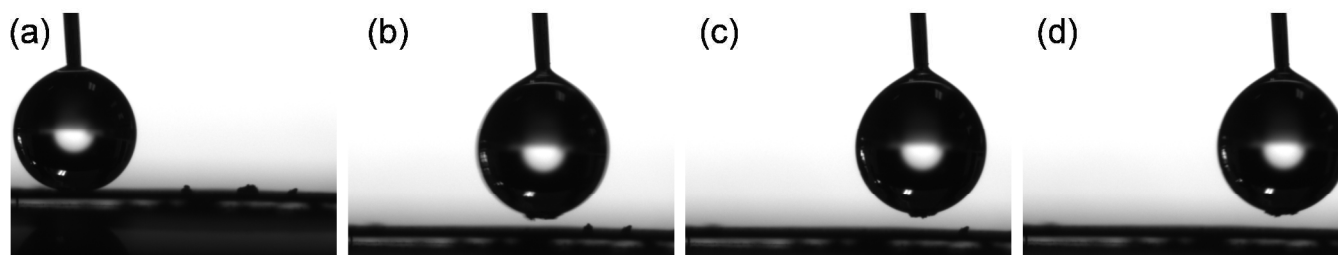


Fig. 6 Demonstration of the self-cleaning effect of the resultant superhydrophobic mesh through the removal of graphite particles from the surface using a moving water droplet (3 μ L)

3.5 Oil/Water Separation

Owing to the robust superhydrophobicity and superoleophilicity, the as-prepared mesh has great potential to separate oil/water mixtures. A series of studies were performed to test the oil/water separation capacities of the as-prepared mesh. The oil/water separation experiment procedure was performed as shown in Fig. 7a and b.⁴⁹ The mesh was fixed between two Teflon fixtures. Both of the fixtures were attached with glass tubes. Since the density of the tested oil petroleum ether is lighter than water, petroleum ether will stay above water. The device was placed obliquely so that petroleum ether could come into contact with the mesh. As pouring the mixture of petroleum ether (dyed with oil red) and water, petroleum ether passed through the mesh with the driving force of gravity, while water was blocked and kept in the upper glass tube.

After the first separation of a petroleum ether/water mixture, the mesh was thoroughly washed with deionized water and performed to successfully separate mixtures of hexane/water, diesel/water, gasoline/water and vegetable oil/water. The separation efficiency of the as-prepared mesh for the series of oil/water mixtures is shown in Fig. 7c, which was calculated by the oil rejection coefficient (R (%)) according to

$$R(\%) = (1 - C_p/C_0) \times 100 \quad (4)$$

Where C_0 and C_p are the oil concentration of the original oil/water mixtures and the collected water after separation, which were measured using the infrared spectrometer oil content analyser. As shown in Fig. 7c, the separation efficiency of the as-prepared mesh for the series of oil/water mixtures is above 99% except for vegetable oil/water. The separation efficiency for vegetable oil (95.95 \pm 0.16%) is a bit lower than the others because of its complex composition and high viscosity.

Because the superhydrophobic layer is robust, the as-prepared mesh can be recycled. The recycling ability was also investigated by taking the petroleum ether/water mixture as an example. After the first separation of a petroleum ether/water mixture, the as-prepared mesh was washed and then used for the same separations. We collected and analysed the samples after 10 and 20 uses. As shown in Fig. 7d, the stability of the as-prepared mesh after 20 uses remained unchanged. In comparison with our former meshes,^{27,49} this facile and fast prepared “oil-removing” mesh likewise has high separation efficiency and good recycling ability, which demonstrates that the as-prepared mesh is another good candidate in industrial oil-polluted water treatment and oil-spill cleanup. Of course, due to its acid and alkali nonresistance, acidic or alkaline oil-polluted wastewater should be neutralized before being treated with the mesh.

4 Conclusions

In this paper, an alkaline-oxidized copper mesh substrate coated quickly with ODPa after immersion in 2×10^{-4} M ODPa/THF solution for 1 second is reported. The ODPa coating was characterized by SEM, FTIR, XPS and contact angle goniometry. It can be verified that the alkyl groups of ODPa layer is not well ordered because the layer forms quickly and the resulting mesh surface exhibits superhydrophobicity with a water CA of 158.9° and superoleophilicity with an oil CA of 0°. Owing to the wetting behaviour, the self-cleaning effect of the mesh was demonstrated and a series of oil/water mixtures such as petroleum ether/water, hexane/water, diesel/water and gasoline/water were performed to be separated by the mesh, the separation efficiency remaining high even after 20 uses. The as-

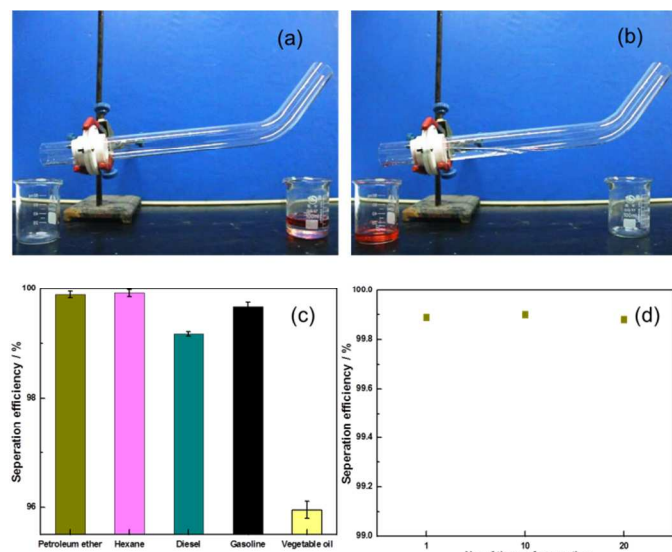


Fig. 7 Oil/water separation studies of the as-prepared mesh: (a) before separation; (b) after separation; and (c) separation efficiency of the mesh for a series of oil/water mixtures; and (d) separation efficiency after 20 times use by taking petroleum ether as an example.

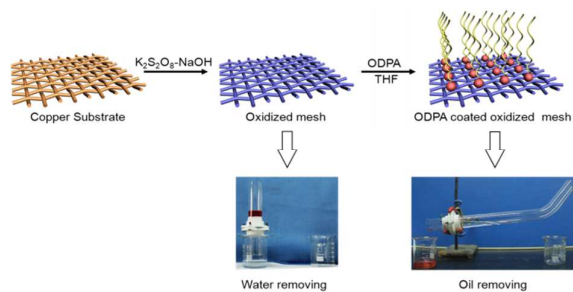
prepared mesh has great potential in industrial oil-polluted water treatment and oil-spill cleanup.

Acknowledgements

Financial support for this work was provided by the National Science Foundation (51173099), the National High Technology Research and Development Program of China (2012AA030306), the National Research Fund for Fundamental Key Projects (2011CB935700), the Fundamental Research Funds for Beijing Jiaotong University (S13JB00100) and the Domestic Visiting Scholar Foundation for Young Core Instructor in Higher Education Institutions from Ministry of Education of PRC. The authors would like to thank Dr. Kan Li in Institute of Chemistry, Chinese Academy of Science for beautiful drawing.

References

- 1 A. Ulman, *An Introduction to Ultrathin Organic Films: From Langmuir–Blodgett to Self-Assembly*, Academic Press, 1991.
- 2 A. Ulman, *Chem. Rev.* 1996, **96**, 1533.
- 3 M. Dubey, T. Weidner, L. J. Gamble and D.G. Castner, *Langmuir*, 2010, **26**, 14747.
- 4 G. Filippini, C. Bonal and P. Malfreyt, *Soft Matter*, 2013, **9**, 5099.
- 5 D. Brovelli, G. Hahner, L. Ruiz, R. Hofer, M. Textor, G. Kraus, A. Waldner, J. Schlosser, P. Oroszlan, M. Ehrat and N.D. Spencer, *Langmuir*, 1999, **15**, 4324.
- 6 P. W. Hoffmann, M. Stelzle and J. F. Rabolt, *Langmuir*, 1997, **13**, 1877.
- 7 E. Hoque, J. A. Derose, B. Bhushan and K.W. Hipps, *Ultramicroscopy*, 2009, **109**, 1015.
- 8 L. Feng, Z. Zhang, Z. Mai, Y. Ma, B. Liu, L. Jiang and D. Zhu, *Angew. Chem. Int. Ed.*, 2004, **43**, 2012.
- 9 M. Nicolas, F. Guittard and S. Geribald, *Angew. Chem. Int. Ed.*, 2006, **45**, 2251.
- 10 T. Ono, T. Sugimoto, S. Shinkai and K. Sada, *Nat. Mater.*, 2007, **6**, 429.
- 11 S. Štandeker, Z. Novak and Ž. Knez, *J. Colloid Interface Sci.*, 2007, **310**, 362.
- 12 J. Yuan, X. Liu, O. Akubulut, J. Xu, S. L. Suib, J. Kong and F. Stellacci, *Nat. Nanotechnol.*, 2008, **3**, 332.
- 13 J. Lahann, *Nat. Nanotechnol.*, 2008, **3**, 320.
- 14 Y. Zhang, S. Wei, F. Liu, Y. Du, S. Liu, Y. Ji, T. Yokoi, T. Tatsumi and F. S. Xiao, *Nano Today*, 2009, **4**, 135.
- 15 X. Gui, J. Wei, K. Wang, A. Cao, H. Zhu, Y. Jia, Q. Shu and D. Wu, *Adv. Mater.*, 2010, **22**, 617.
- 16 G. Hayase, K. Kanamori and K. Nakanishi, *J. Mater. Chem.*, 2011, **21**, 17077.
- 17 Y. L. Zhang, H. Xia, E. Kim and H. B. Sun, *Soft Matter*, 2012, **8**, 11217.
- 18 U. Manna, A. H. Broderick and D. M. Lynn, *Adv. Mater.*, 2012, **24**, 4291.
- 19 G. Hayase, K. Kanamori, M. Fukuchi, H. Kaji and K. Nakanishi, *Angew. Chem. Int. Ed.*, 2013, **52**, 1.
- 20 X. F. Huang and T. T. Lim, *Desalination*, 2006, **190**, 295.
- 21 C. Lee and S. Baik, *Carbon*, 2010, **48**, 2192.
- 22 L. F. Wang, S. Y. Yang, J. Wang, C. F. Wang and L. Chen, *Mater. Lett.* 2011, **65**, 869.
- 23 J. Wu, J. Chen, K. Qasim, J. Xia, W. Lei and B. P. Wang, *J. Chem. Technol. Biotechnol.* 2012, **87**, 427.
- 24 D. D. Nguyen, N. H. Tai, S. B. Lee and W. S. Kuo, *Energy Environ. Sci.* 2012, **5**, 7908.
- 25 P. Thanikaivelan, N. T. Narayanan, B. K. Pradhan and P. M. Ajayan, *Sci. Rep.* 2012, **2**, 230.
- 26 Z. X. Xue, S. T. Wang, L. Wang, L. Lin, L. Chen, M. J. Liu, L. Feng and L. Jiang, *Adv. Mater.* 2011, **23**, 4270.
- 27 N. Liu, Y. Chen, F. Lu, Y. Cao, Z. Xue, K. Li, L. Feng and Y. Wei, *ChemPhysChem.*, 2013, **14**, 3489.
- 28 J. T. Woodward, A. Ulman and D. K. Schwartz, *Langmuir*, 1996, **12**, 3626.
- 29 I. Doudeviski, W. A. Hays and D. K. Schwartz, *Phys. Rev. Lett.*, 1998, **81**, 4927.
- 30 D. K. Schwartz, *Annu. Rev. Phys. Chem.*, 2001, **52**, 107.
- 31 B. R. A. Neves, M. E. Salmon, P. E. Russell and E. B. Troughton, *Langmuir*, 2000, **16**, 2409.
- 32 B. R. A. Neves, M. E. Salmon, E. B. Troughton and P. E. Russell, *Nanotechnology*, 2001, **12**, 285.
- 33 H. -Y. Nie, M. J. Walzak and N. S. McIntyre, *Langmuir*, 2002, **18**, 2955.
- 34 H. -Y. Nie, D. J. Miller, J. T. Francis, M. J. Walzak, and N. S. McIntyre, *Langmuir*, 2005, **21**, 2773.
- 35 T. Keszthelyi, Z. Paszti, T. Rigo, O. Hakkell, J. Telegdi and L. Guzzi, *J. Phys. Chem. B*, 2006, **110**, 8707.
- 36 M. M. Antonijevic and M. B. Petrovic, *Int. J. Electrochem. Sci.*, 2008, **3**, 1.
- 37 W. Guo, S. Chen and H. Ma, *J. Serb. Chem. Soc.*, 2006, **71**, 167.
- 38 G. John and V. Alsten, *Langmuir*, 1999, **15**, 7605.
- 39 C. M. Whelan, M. Kinsella, H.M. Ho and K. Maex, *J. Electrochem. Soc.*, 2004, **151**, B33.
- 40 Y. S. Tan, M. P. Srinivasan, S. O. Pehkonen and S. Y. M. Chooi, *J. Vac. Sci. Technol. A*, 2004, **22**, 1917.
- 41 R. Tremont, H. De Jesus-Cardona, J. Garcia-Orozco, R. J. Castro and C. R. Cabrera, *J. Appl. Electrochem.*, 2000, **30**, 737.
- 42 A. M. Skolnik, W. C. Hughes and B. H. Augustine, *Chem. Educator*, 2000, **5**, 8.
- 43 P. E. Laibinis and G. M. Whitesides, *J. Am. Chem. Soc.*, 1992, **114**, 9022.
- 44 C. Gao, Z. Sun, K. Li, Y. Chen, Y. Cao, S. Zhang and L. Feng, *Energy Environ. Sci.*, 2013, **6**, 1147.
- 45 S. Nishimoto, A. Kubo, K. Nohara, X. Zhang, N. Taneichi, T. Okui, Z. Liu, K. Nakata, H. Sakai, T. Murakami, M. Abe, T. Komine and A. Fujishima, *Appl. Surf. Sci.*, 2009, **255**, 6221.
- 46 S. Marcinko and A. Y. Fadeev, *Langmuir*, 2004, **20**, 2270.
- 47 H.-Y. Nie, M. J. Walzak and N. S. McIntyre, *J. Phys. Chem. B*, 2006, **110**, 21101.
- 48 X. Zhang, Z. Li, K. Liu and L. Jiang, *Adv. Funct. Mater.*, 2013, **23**, 2881.
- 49 Y. Cao, X. Zhang, L. Tao, K. Li, Z. Xue, L. Feng and Y. Wei, *ACS Appl. Mater. Interfaces*, 2013, **5**, 4438.



Simple and fast method to prepare superhydrophobic octadecylphosphonic acid (ODPA) coating on oxidized copper mesh for oil/water separation.